International Journal of Scientific Engineering and Technology (ISSN : 2277-1581)
Volume No.3 Issue No.8, pp : 1119-1122 1 Aug 2014

Design and Analysis of Tunable Infrared Photodetector Using Defect Based 1D Photonic Crystal

Alireza Mobini

Faculty of Electrical Engineering, Qom University of Technology, Qom, Iran
mobini@qut.ac.ir

Abstract: ***In this work, a defect based photonic crystal (PC) structure presented for design of tunable infrared photodetector. Absorption response was investigated under the effects of various structural parameters. Using straight transfer matrix method, PC band edge effect was studied on absorption and a significant absorption enhancement up to %96 was achieved for defect-based structure.***

Keywords: Infrared Photodetector, Photonic Crystal, TMM.

1. Introduction

Infrared (IR) photodetectors are extremely important in wide area of applications such as environmental monitoring, combustion exhausted efficiency [1-3], remote identification of chemical and biological compounds [4], thermal imaging sensors, sallow night vision, surveillance products, building inspection and anomaly detection [5-8]. There are different technologies for a different range of detection wavelength as an example poly-Si metal–insulator–semiconductor and GaN/Si based detector for ultraviolet, telluride-based semiconductors for terahertz and quantum well and dot for IR range [9-12]. Over the past years, huge efforts have been done for improvement of IR photodetectors characteristics using different processes and structures like a photonic crystal (PC), metallic array, DBR layers and nonlinearity [12-13]. Photonic crystal structure with periodic array of different dielectric materials perturbs propagating frequency modes and causes occurrence of photonic band gaps (PBG) [14]. The resulted band edge mode with low group velocity effect is utilized for manipulating of lasing and absorbing gain of active layer [15]. Studies on gain characteristics of PBG structures are focused on low-threshold laser presented in numerous papers [15-16] and absorbing gain under effect of 2D photonic crystal, discussed in some references [17-18].

There are a variety of numerical methods like a plane wave expansion (PWE), finite difference time domain method (FDTD), finite difference frequency domain (FDFD), and transfer matrix method (TMM) for studding propagation of light in PC structures [19-22]. TMM used in this work, is a well-known method for solving Maxwell's equation in 1D structures. This method is competitive with other methods such as PWE and FDTD. Comparison between these methods reveals that TMM results are in good agreement with experimental results, especially for 1D PC [23].

In this work, multilayered dielectric structure, known as 1D PC, was analyzed for designing tunable IR photodetector. Structural parameters including non-absorptive layer refractive index, number of top and bottom layers and defect layer thickness were completely analyzed and classified. This regular classification yields some rules for designer to design higher performance IR photodetector. The results were used for exact tune of peak response location in IR spectrum. A significant enhancement up to %96 was observed in absorption coefficient using these structures.

The rest of this paper is organized as follows. In section 2, the simulation method used in this work explained. In section 3 parameters of defect-based structure has been presented for designing IR photodetector.

2. Numerical Method

TMM is a well-known method for solving Maxwell's equations for investigating electromagnetic wave propagation in 1D PC. This method was applied in the present study for calculation of scattering parameters i.e. transmission, reflection, and absorption coefficients of 1D PC-based photodetector. In this method, the electrical field is considered as sum of two transmitted and reflected wave components [23-25]:

$$E(z,\omega) = E_t e^{ik.z} + E_r e^{-ik.z} \quad (1)$$

In this work, structure was divided into N segments and then Maxwell boundary equations were applied to each segment. Based on this method, for a propagation of wave through two segments, two matrixes are inserted: P_i and I_i. P_i is for wave propagation in each segment as continuum environment and I_i is for a propagation of wave in interface of two adjacent segments. Finally, total transfer matrix M was calculated using P_i and I_i, as:

$$M = I_{2n+1} \prod_{i=1}^{2n} P_i I_i \quad (2)$$

In this method, absorption coefficient was calculated from difference of all input power from sum of transmission and reflection coefficients, T and R, respectively. T and R were calculated from Eq. (3) and Eq. (4), respectively:

$$T = \left| M_{11} - M_{12} M_{21} / M_{22} \right|^2 \quad (3)$$

$$R = \left| M_{21} / M_{22} \right|^2 \quad (4)$$

Where, M_{ij} is M matrix element.

International Journal of Scientific Engineering and Technology (ISSN : 2277-1581)
Volume No.3 Issue No.8, pp : 1119-1122 1 Aug 2014

3. Simulation and Results

3.1. *1D Photonic Crystal*

Schematic of 1D PC constructed from *N* periods of different dielectric materials is shown in Fig .1(a). Layers have refractive index and thickness of n_1, d_1 and n_2, d_2, respectively. The total thickness of device is $N(d_1+d_2) + d_s$, where d_s is substrate thickness.

The thickness of each individual layer for a certain central wavelength in IR spectrum (λ_0) can be calculated from Eq. (5):

$$d_i = \frac{\lambda_0}{4 \times n_i} \quad (5)$$

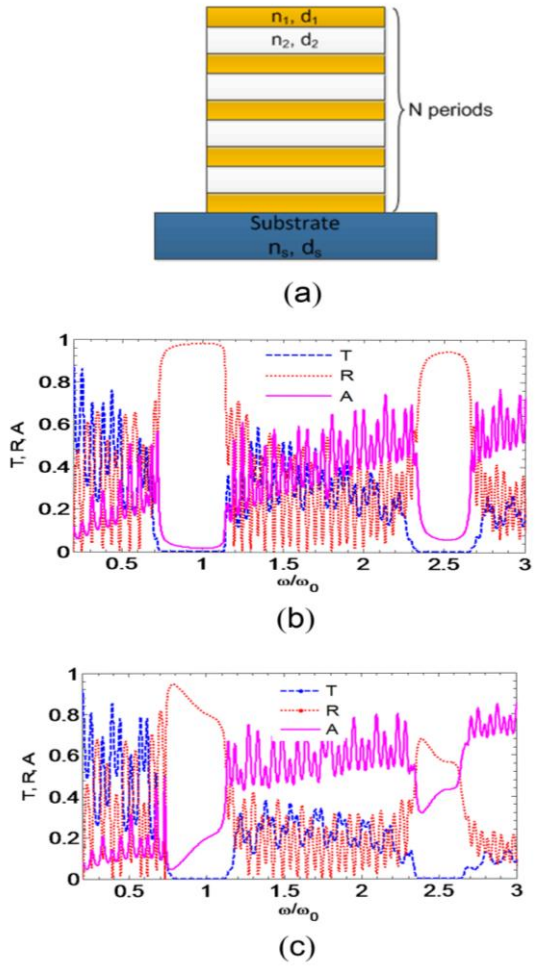

Fig. 1. (a) Schematic of PC structure used for IR photodetector. Transmission, reflection and absorption coefficients of 1D PC for IR photodetector for a (b) S_1 structure with $n_1=3.55+i0.035$ and $n_2=1.7$ and (c) S_2 structure with $n_1=3.55+i0.035$ and $n_2=5.5$.

ɔn is
ple of
ld be

selected small enough that the incoming wave in IR spectrum sees the changing of dielectric longitudinally and also computer simulation load does not ineffectually increase.

The coupling effect from source medium, air in this example, to structure and coupling wave from device to environment were considered as two P_0 and P_n matrixes, respectively.

3.2. *1D Photonic Crystal IR Absorption Spectrum*

When inserting absorptive region (yellow layers in Fig .1(a)), the imaginary part of refractive index causes absorption of incident wave in device while propagating through it. Results were considered for two structures with different refractive indices. For a first structure (S_1) the non-absorptive layer has smaller refractive index than absorptive layer refractive index means: $n_1=3.55+i0.035$ and $n_2=1.7$. For the second structure (S_2), non-absorptive layer has greater refractive index than absorptive layer refractive index, as $n_1=3.55+i0.035$ and $n_2=5.5$. For these two structures, scattering parameters transmission, reflection and absorption coefficients were calculated and presented in Fig. 1(b) and Fig. 1(c).

As understood from Fig. 1, all three coefficients are changing concurrently. This means that when one of the coefficients decreases or increases the other ones increase or decrease. For example for $n_2=5.5$, in frequency range of $1.12\omega_0 \le \omega \le 2.3\omega_0$ that absorption coefficient increases, the reflection and transmission coefficients decrease. In addition, comparing refractive indices in S_1 and S_2, it was observed that in S_2 refractive indices ratio of two sequential layers decreases and results in a decrease in Bragg effect. Therefore, it can be stated that absorption coefficient increases in high frequencies. In smaller frequencies, wavelengths increase and the incoming light sees periodicity of structure poorly, resulting in weak Bragg effect, thus transmission increase.

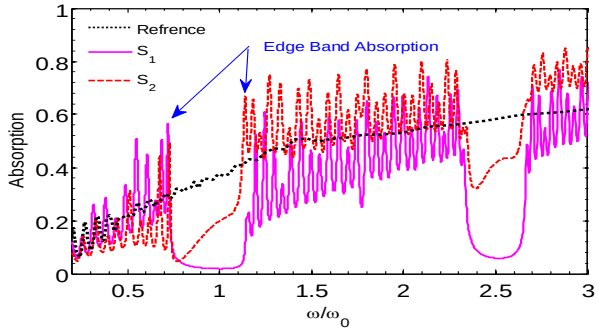

Fig. 2. Absorption coefficient of S_1, S_2 and reference structures.

Also, absorption coefficient for S_1, S_2 and reference structure shown in Fig .2. There is edge band enhanced absorption for S_1 and S_2 structures as shown in Fig .2. As depicted in this figure, because of wave energy concentration, absorption enhancement occurs in lower frequencies at band edge when refractive index of absorptive material is higher than non-absorptive material (i.e. in S_1 structure). In this way, absorption enhancement occurs in higher frequencies in band edge, when the refractive index of absorptive material is lower than non-absorptive material (i.e. in S_2 structure).

3.3. *IR Absorption Spectrum of 1D Photonic Crystal with Defect layer*

For fine tune of absorption response in certain wavelength in IR spectrum, a defect layer is inserted into the structure [26-27]. The defect layer was selected from absorptive layer type. By adding this defect layer, comparing with Fig. 1(b) and Fig. 1(c),

the absorption gap around λ_0 vanishes and new absorptive modes arises that changes with changing structural parameters. Using this property, the effect of different structural parameters (e.g. refractive index of non-absorptive layer, defect layer thickness and number of bottom and top layers) regularly were examined for design of tuned photodetector. This range of designing parameters allows designers to exactly tune the absorption response peak location for various applications.

3.3.1. *Changing Number of Layer Under the Defect Layer*

The effect of bottom layer numbers (N_r) in absorption response is shown in Fig. 3(a). These layers are located under the defect layer. As shown in the figure, for small values of N_r the amplitude of peak is decreased since the incoming light can escape easily from defect region to substrate without being absorbed. For greater values of N_r, light cannot escape and is more confined and eventually absorbed. For N_r=10 absorption reaches 0.92 and finally for N_r=20 absorption saturates with maximum value and there is no need for further raise of this parameter. There is little difference between absorption for N_r=10 and N_r=20; however, for the smaller values of N_r, device has shorter length. Thus, the value of N_r=10 is selected as the optimum value.

3.3.2. *Changing Number of Layers Above the Defect Layer*

The effect of top layer numbers (N_l) in absorption response is shown in Fig. 3(b). As shown in this figure, for small values of N_l, the amplitude of peak is decreased due to the weak effect of Bragg scattering, on the other hand, once the number of top layer was increased, i.e. N_l =8, the incoming wave highly reflected and cannot inter to the structure and reach absorptive region. Therefore, there is a tradeoff between Bragg scattering effect and input power value that reaches absorption area. As shown in Fig. 3(b), for range of 2-8, N_l=4 is proper value for designing, as for this value absorption peak get maximum (shown in blue color in Fig. 3(b)).

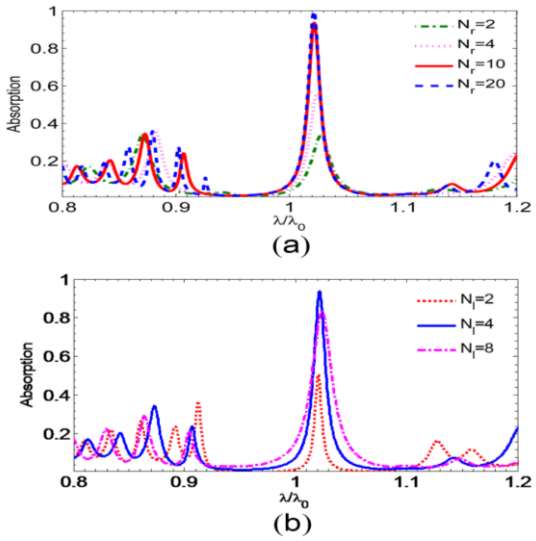

Fig. 3. (a) Absorption response of PC for IR photodetector for different number of bottom layer and N_l =4 (b) Absorption response of PC for IR photodetector for different number of top layer and N_r =10.

3.3.3. *Changing Refractive Index of non-absorptive Layer*

The effect of non-absorptive layer refractive index (n_2) in absorption response illustrated in Fig. 4(a). This parameter varies gradually in the range of 2 to 5.5. For value of 2, there is no notable peak in absorption response. When n_2 equals to 2.6, a considerable peak appears in response. This peak has a blue shift with increasing n_2 and finally disappeared at n_2=3.4 and then another peak showing itself at greater wavelength. This new peak becomes dominant peak in absorption response for values greater than n_1.This peak is depicted in Fig. 4(a) in pink color for n_2=5.5.

3.3.4. *Changing Defect Layer Thickness*

Another important parameter for designing a defect PC-based photodetector is defect layer thickness (t_d). Fig. 4(b) shows the effect of this parameter on absorption. Generally speaking, when the absorptive layer thickness increases the

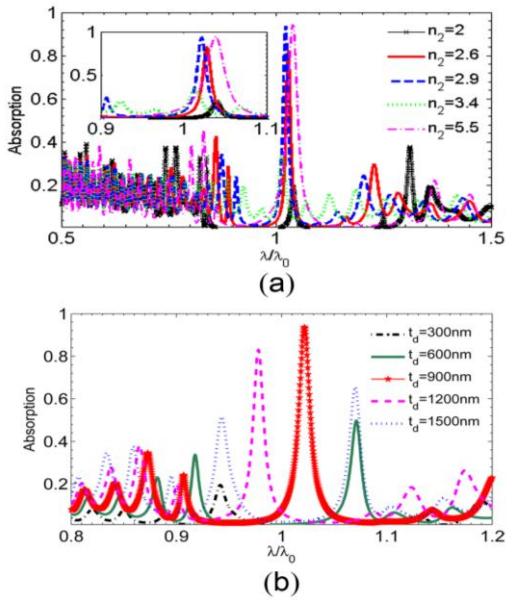

Fig. 4. (a) Absorption response of PC for IR photodetector for different value of non-absorptive layer refractive index and (b) Absorption response of PC for IR photodetector for different value defect layer thickness. absorption coefficient will also increase, because of more absorptive material. However, this absorption probably does not occur in certain wavelength for desired application. Accordingly, it is required to find the optimum value of t_d leading to the most amount of absorption in cavity mode. As shown in Fig. 4(b), the defect layer thickness varies gradually from 300nm to 1500nm. As illustrated in the figure, for d_d=300nm, there is a week defect mode with week amplitude. An increase in thickness of defect layer results in the increasing absorption peak amplitude, where at d_d=900 nm, there is a strong defect mode in 1D PC structure resulting in higher peak value in absorption response (shown in red color in Fig. 4(b)). After this value (d_d=900 nm), the absorption peak amplitude decreases and finally vanishes. Thus d_d=900 nm is the optimum value here.

4. Conclusion

In this paper, defect-based PC was used for designing IR photodetector. Using TMM method, the effects of structural parameters including were investigated. Utilizing the obtained results, a significant absorption coefficient was obtained up to %96. Results showed there is a blue shift in absorption mode with increasing non-absorptive layer refractive index that can be used for tuning of absorption mode.

References

i. S. Pal, K.B. Ozanyan, and H. McCann, J. of Phys. Conf. Ser. 85, 012020 (2007).
ii. U. Willer, M. Saraji, A. Khorsandi, P. Geiser, and W. Schade, Optics and Lasers in Engineering 44, 699 (2006).
iii. K-K. Choi, The Physics of Quantum Well Infrared Photodetectors (World Scientific, Singapore, 1990).
iv. J. P. Kerekes, M. K. Griffin, J. E. Baum, and K. E. Farrar, Modeling of LWIR hyperspectral system performance for surface object and effluent detection applications— Proc. of Algorithms for Multispectral, Hyperspectral, and Ultraspectral Imagery VII (SPIE, Florida, 2001), pp. 348–359.
v. L-M. Kong, J. Zhang, X-K. Cheng, C-X. Zhang, and R. Wang Modern Physics Letter B 23, 3265 (2009).
vi. J. Vaillancourt, P. Vasinajindakaw, and X. Lu, Optics and Photonics Letters 4, 57 (2011).
vii. P. Norton, Opto-Electronics Review 14, 1 (2006).
viii. C. A. Balaras and A. A. Argiriou, J. Energy and Buildings 34, 171 (2002).
ix. Y. Zhou and Y. He International Journal of Modern Physics B 25, 2403 (2011).
x. Z. Ye, X. Gu, J. Huang, Y. Wang, Q. Shao, and B. Zhao, International Journal of Modern Physics B 16, 4310 (2002).
xi. D. Khokhlov, International Journal of Modern Physics B 18, 2223 (2004).
xii. A. Mobini and V. Ahmadi IEEE J. of Photonic Tech. Lett. 26, 1231 (2014).
xiii. H. C. Liu, E. Dupont, and M. Ershov, J. of Nonlinear Optical Physics & Materials 11, 433 (2002).
xiv. Ph. St. J-Russell, T. A. Birks, and F. D. Lloyd-Lukas, Photonic Bloch waves and photonic band gaps, (Plenum Press, New York, 1995).
xv. K. Sakoda, Opt. Express 4, 167 (1999).
xvi. K. Sakoda, Kazuo Ohtaka, and Tsuyoshi Ueta, Opt. Express 4, 481(1999).
xvii. Z. Ku et al, Opt. Express 21, 4709 (2013).
xviii. S. Kalchmair, H. Detz, G.D Cole, A.M Andrews, P. Klang, M. Nobile, R. Gansch, C. Ostermaier, W. Schrenk, and G. Strasser, J. Appl. Phys. Lett. 98, 011105 (2011).
xix. J. B. Pendry and A. MacKinnon, Phys. Rev. Lett. 69, 2772 (1992).
xx. J. B. Pendry, J. of Phys.: Condens. Matter 8, 1085 (1996).
xxi. J. Arriaga, A.J. Ward, and J.B. Pendry, Phys. Rev. B 59, 1874 (1999).
xxii. A. Taflove, IEEE Trans. Electro. Compat. 22, 191 (1980).
xxiii. J. B. Chen, Y. Shen, Wei-Xi Zhou, Yu-Xiang Zheng, Hai-Bin Zhao, and Liang-Yao Chen, J. of the Korean Physical Society 58, 1014 (2011).
xxiv. W. Zhou, L. Chen, H.Yang, and G. J. Brown Journal of Nanophotonics 1, 013515 (2007).
xxv. J. D. Joannopoulos, S. G. Johnson, J. N. Winn, and R. D. Meade, Photonic Crystals: Molding the Flow of Light, 2nd edition: (University Press, Princeton, 2008).
xxvi. Alvarado-Rodriguez et al, J. of applied physics 92, 6399 (2002).
xxvii. Temelkuran, B., E. Ozbay, J. P. Kavanaugh, G. Tuttle, and K. M. Ho, Appl. Phys. Lett. 72, 2376 (1998).
xxviii. J. P. Vigneron and V. Lousse, Springer Optical and Quantum Electronics 39, 377 (2007).
xxix. C. J. Wu and Z.H. Wang, Progress In Electromagnetics Research 103, 169 (2010).
xxx. M. Renilkumar and P. Nair, Elsevier Optical Materials 33, 53 (2011).